

Chapter 3: Vacuum Technology

Table of contents

3.1. Pump selection and exhaust handling;

3.2. Problem gases;

3.3. Gas throughput;

3.4. Contamination sources:

3.4.1. Oil backstreaming;

3.4.2. Gas evolution;

3.4.3. Dust;

3.5. Pressure measurement;

3.6. Conclusion;

Most thin film deposition processes happen in an environment that is different from the atmospheric ambient. Vacuum pumps and enclosures (chambers) are needed to create such an environment (see Fig. 3.1).

36 Vacuum Technology

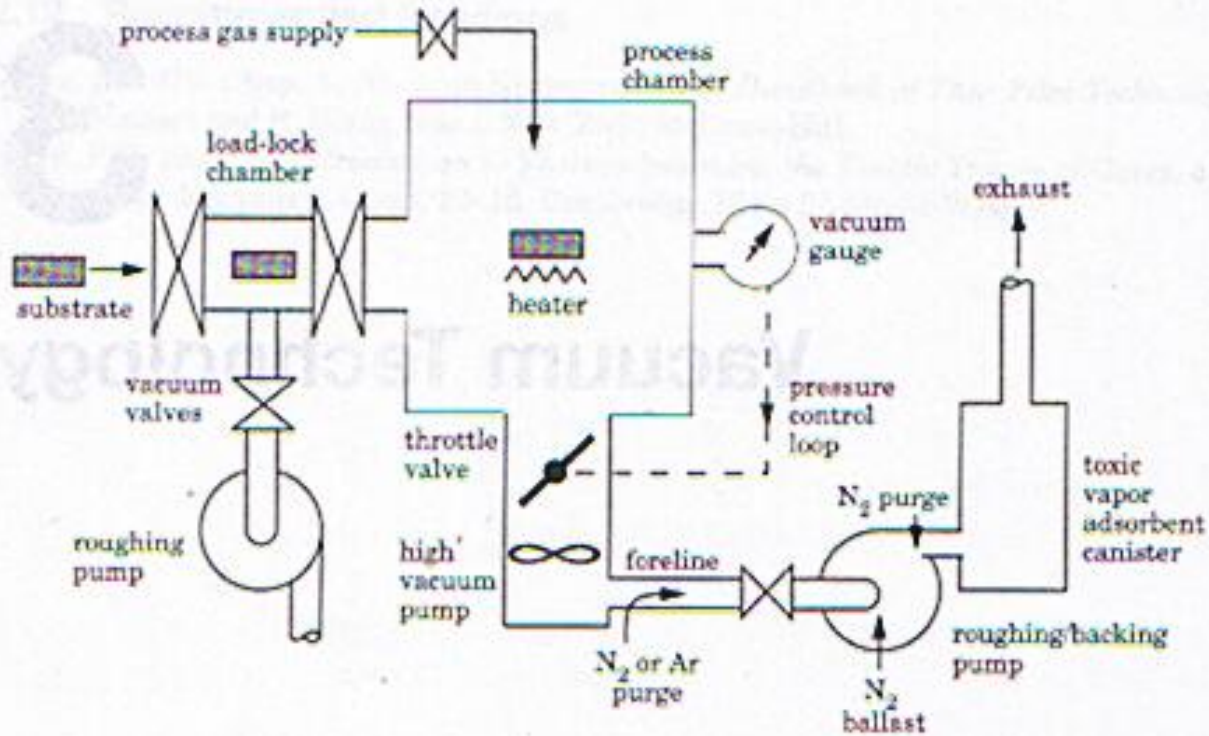


Figure 3.1 Typical vacuum-system components for thin-film deposition.

TABLE 3.1 Vacuum Pump Characteristics

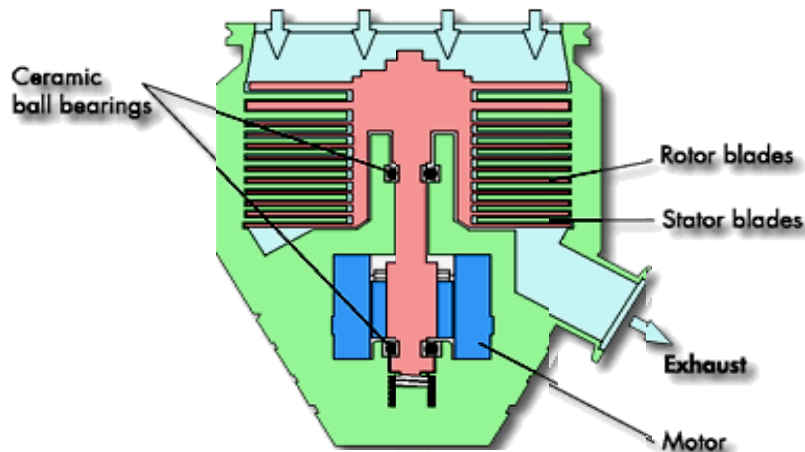
Pressure ranges	Name	Category	Approx. \$/l/s	Backing pump req'd?	Oil present?		Problematic gases and vapors	Other comments
					Inlet	Outlet		
	Dry rotary	Displacement	1000	No	No	Yes	Condensables require gas ballasting; see text	Common for roughing/backing
	Oil-sealed rotary		300	No	Yes	Yes		
	Roots blower		70	Yes	No	Yes	Low compression ratio for H ₂ and He	Oil contam. unless foreline purged
	Molecular drag		35	Yes	No	Yes*		
	Turbo-molecular		40	Yes	No	Yes*		
	Oil diffusion		5	Yes	Yes	Yes	Explosion danger with flammables	Greatest risk of oil contam.
	Cryosorption		450	No	No	(No outlet)		For dry roughing
	He-cycle cryopump	7	No	No	No†	Low capacity for He, H ₂		
	Sputter-ion	25	No	No	(No outlet)	Poor for inerts		
	Flow regime for 5 cm diameter tube log of pump inlet pressure -10 -5 -5 0 0 Torr +5 Pa 1 atm molecular ← transition → fluid							

*except magnetically levitated bearing types, which use no lubrication
 †Purge roughing pump line to avoid oil contamination during warmup/regeneration cycle.

The true function of all pumps: to create a pressure difference between the inlet and the outlet;

Turbomolecular pump

The ATP standard version cross section



www.west-technology.co.uk

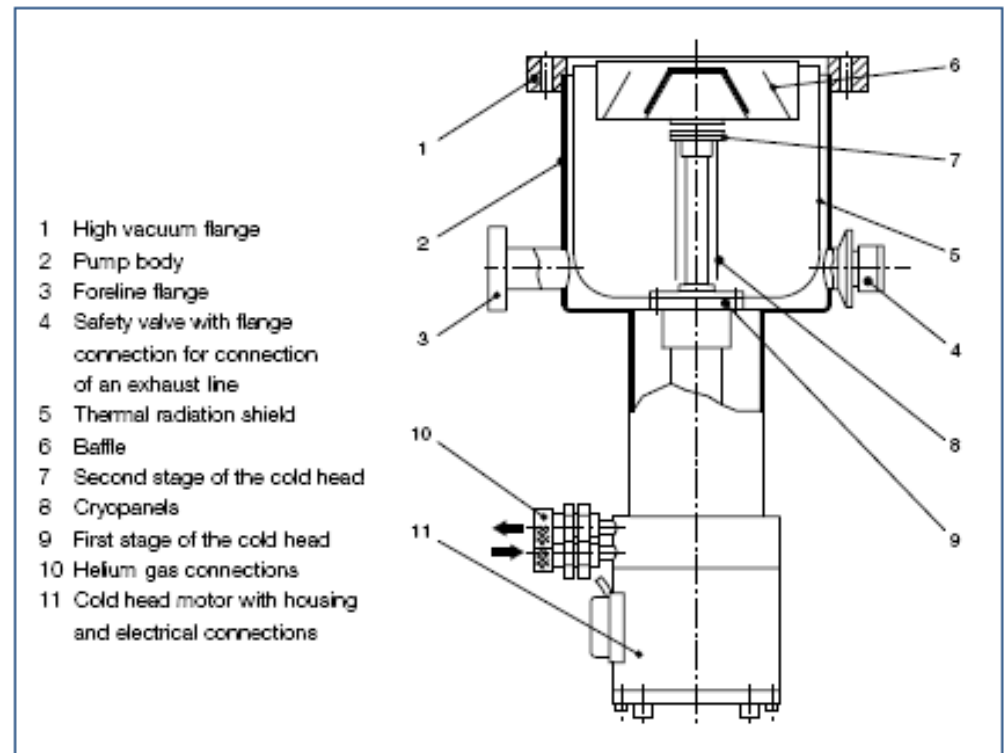
1. Pumping principle: *displacement*;
2. very high blade rotation speed (20,000-90,000 rpm)
3. multiple stage operation;
4. typically requires a fore-pump;
5. The downward angle of the rotor blades results in most of the scattered molecules to leave them in downward direction
6. Operating pressure limits:
 - High pressure: the very short mean free path of gas molecules demand the spacing between rotor blades be too small to be practical, plus the excessive resistance the blades experience;
 - Low pressure: speed of the rotor and the relative area of the pump opening to that of the chamber surface;

Cryopumps

1. Pumping principle: condensation / *trapping*;

2. Operating pressure limits:

- High pressure: massive condensation and the limited thermal conductivity of the condensed gas makes the temperature of the outer surface of the condensed gases too high;
- Low pressure: the high vapor pressure of selected gases such as He and H₂;



COOLVAC refrigerator cryopump

3.3 Gas Throughput of pumping systems

3.3.1 The mass flow of gases must satisfy the continuity equation:

$$\text{Input} + \text{generation} = \text{output} + \text{accumulation}$$

Where generation refers to gas desorption or production; accumulation means pressure buildup and condensation. All the mass flow quantities are expressed in units of volume times the pressure and divided by time.

In a typical system, the output is composed of three consecutive parts: **throttle constriction, pipe conductance, and the pumping speed.**

3.3 Gas Throughput of pumping systems (cont'd)

- Referring to Fig. 3.3, we have: $Q_s + Q_i \approx Q_s = C_2(p_2 - p_1) = C_1(p_1 - p_o) = C_o P_o$
where the throughput across any constriction is in the form of $Q = C\Delta p$; and C is known as the conductance or the pumping speed. Q is in units of pressure \times volume/time, e.g. Pa L/s or torr L/s. These units are proportional to mc/s **with a multiplication factor of kT** .
- Note that pump throughput Q is different from the commonly encountered **pumping speed** in L/s.
- For a pump, we have $\Delta p \approx p_o$ at the inlet. This is because that the pressure inside a pump is assumed to be much lower than the lowest pressure that can be achieved at its inlet.

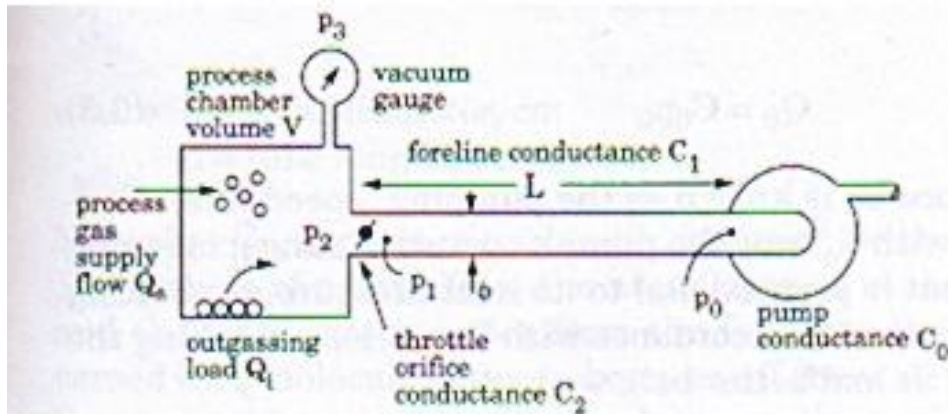


Figure 3.3 Geometry for gas throughput calculations.

An alternative and commonly used unit for Q : standard cubic centimeters per minute (sccm). It stands for the flow of 1 cc of gas under standard condition, i.e. 1 atm in one minute time.

3.3.2. Derivation of $Q = C\Delta p$ for an orifice in molecular flow regime:

Assuming the pressure on the two sides of the orifice is p_1 and p_2 , respectively:

$$Q_2 = (J_{i2} - J_{i1}) \cdot A$$

From Knudsen equation (Eq. (2.18)), i.e. J_i as a function of p , we have:

$$Q_2 = \frac{N_A}{\sqrt{2\pi MRT}} A(p_2 - p_1) \equiv AC_A(p_2 - p_1) = C_2(p_2 - p_1)$$

For air at room temperature:

$$C_A \equiv \frac{C_2}{A} = 11.6 \text{ litre/sec}\cdot\text{cm}^2$$

$$C_A \equiv \frac{C_2}{A} = 11.6L/\text{sec}\cdot\text{cm}^2 = 8.06/Pa\cdot\text{sec}$$

3.3.2. Derivation of $Q = C\Delta p$ for an orifice in molecular flow regime: (cont'd)

The above derivation applies to an orifice in molecular flow, i.e. the molecular mean free path is larger than the orifice diameter. In viscous flow case, C_A is much larger and therefore less likely to be a limiting factor in the entire line of gas flow. In the meantime, its derivation is also more complex.

Note that the maximum pump throughput decreases with decreasing pressure since the maximum value of $p_2 - p_1$ is p_2 , and if p_2 is orders of magnitude lower, than Q is orders of magnitude lower despite the pumping speed being at a constant.

3.3.3. The function of a throttle valve:

Control the pressure distribution at various points within a vacuum system, i.e. imposing a C_t that causes the pressure on the two sides to be different. The larger the C_t , the smaller the pressure difference that will be needed to fulfill the gas flow continuity requirement.

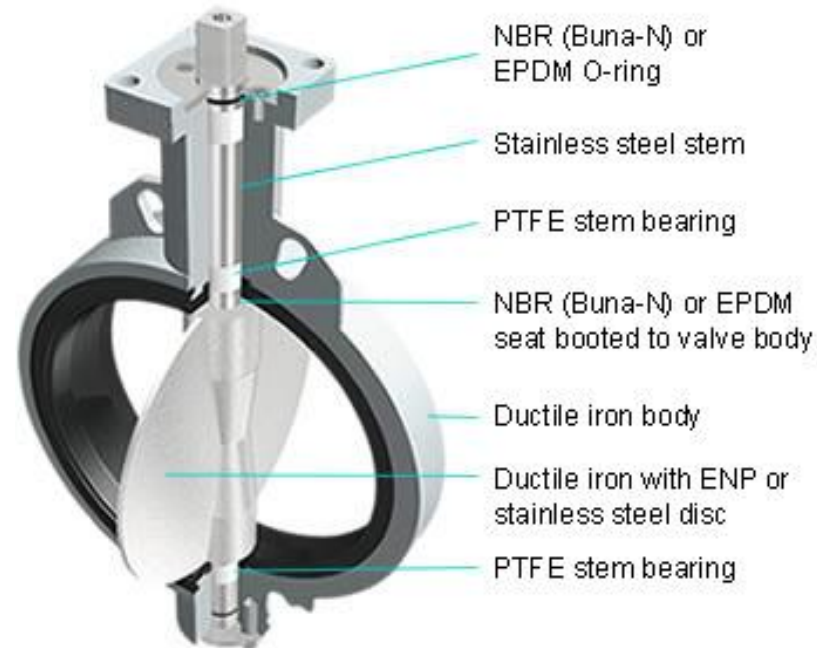


* Illustration shows 14" & larger sizes

3.3.4. Conductance of air-through long tubes:

$$C_m = 12.3\phi^3 / L$$

$$C_v = 1.41\phi^4 \bar{p} / L$$

where **m** and **v** refer to molecular and fluid flow regimes, respectively;

3.3.5. Example: the rate of pumping down from 1 atm.

Assuming Q_i & $Q_s \approx 0$, i.e. the gas load due to both the desorption from the chamber wall and the supply rate of process gas are zero; p_2 is the chamber pressure which is also the pressure at the inlet of the pump. We get from the continuity equation, the rate of removal of gas molecules from a volume V should equal to the pumping speed, i.e.,

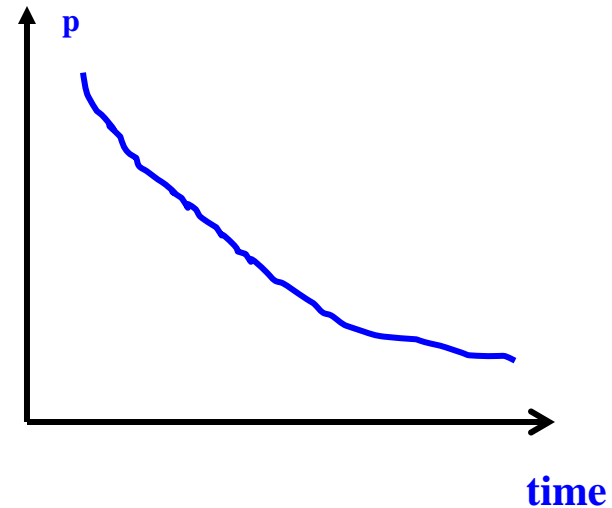
Input + generation = output + accumulation

$$0 + 0 = C_o p_2 + V \frac{dp_2}{dt}$$

$$\therefore -\frac{C_o}{V} dt = \frac{dp_2}{p_2}$$

$$\therefore p_2 = p_{20} \exp\left(\frac{-t}{V/C_o}\right)$$

where $p_2 = p_{20}$ at $t = 0$



3.3.5. Example: the rate of pumping down from 1 atm (cont'd)

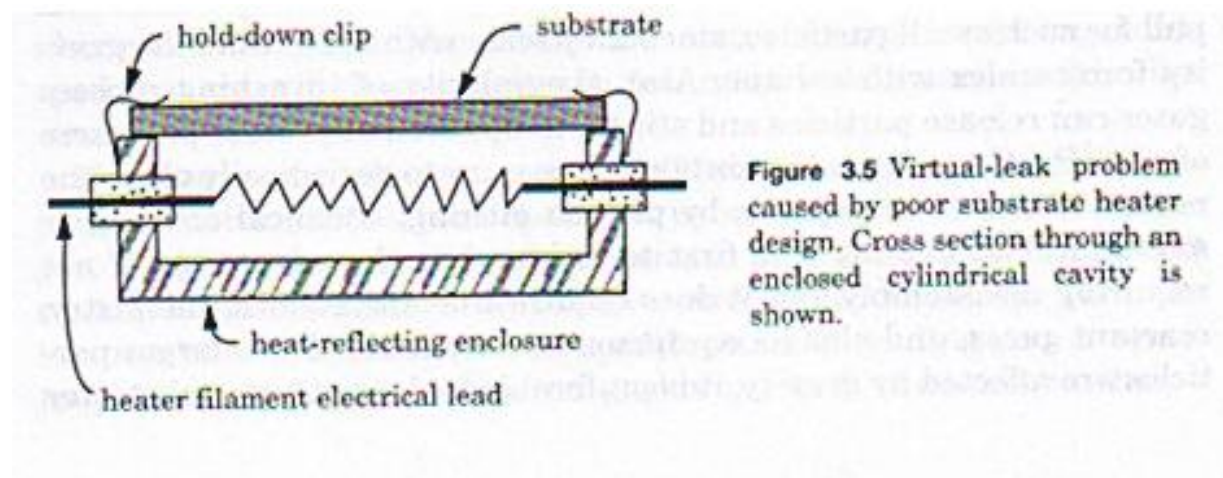
Therefore, p_2 decays in an exponential fashion with time. The decay time constant is V/C_0 . It is intuitively apparent that for a given volume V , the higher the pumping speed, the faster the pressure reduces.

In reality, the equation is valid down to a pressure of ~ 10 Pa, below which outgassing from the chamber wall becomes a non-negligible factor. As a result, differential equation will have to be changed to reflect the fact that Q_i is no longer zero; for even lower pressure, the reduction in the pumping speed could also take effect.

3.3.6. Considerations for choosing the tube size for the connection between the chamber and the pump: Larger diameter tubing reduces the pressure drop along the tube, allowing for maximizing the pump's function. However, large diameter tubing is associated with large surface area, and therefore larger outgassing. A compromise will have to be established.

3.4.4. Gas evolution

- Chamber wall outgassing
- Gas permeation: through elastomer O-ring
- Presence of high vapor pressure materials
- Virtual leak: trapped gas



3.5. Pressure Measurements

We will talk about two types of pressure gauges: thermocouple, and capacitance diaphragm (see Fig. 3.6).

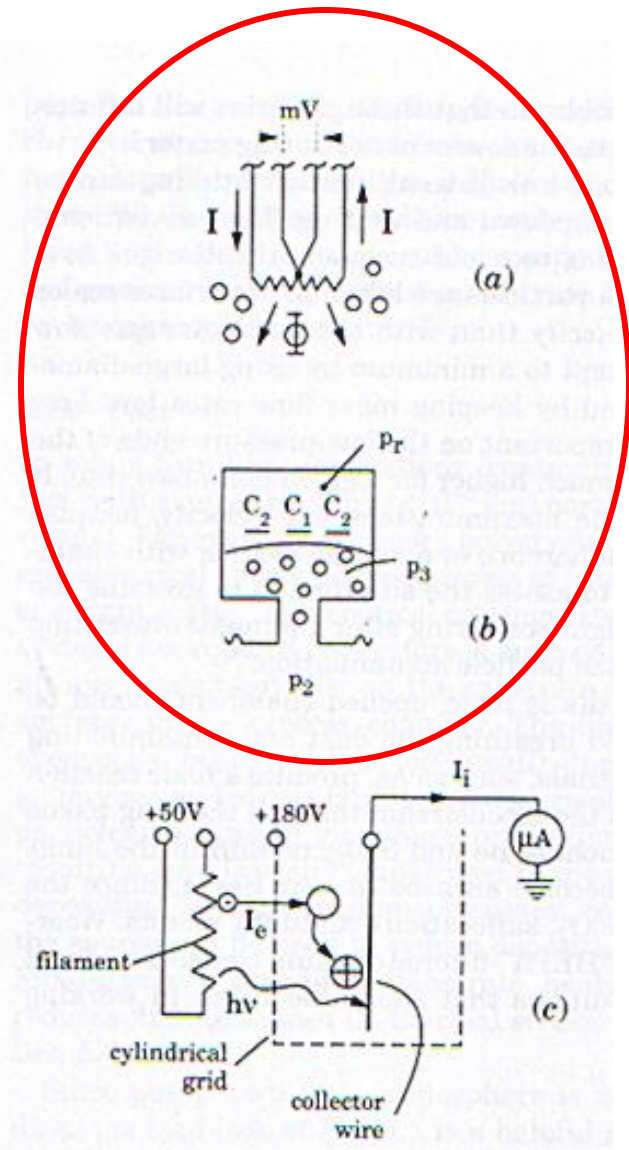


Figure 3.6 Vacuum-gauge operating principles: (a) thermocouple gauge, (b) capacitance diaphragm gauge, and (c) ion gauge.

3.5.1. Thermocouple gauge:

- Operational principle: $K_n > 1$ is always satisfied thus $h_c \sim p$. With a calibrated dial, pressure measurement is possible.
- Nonlinear; gas composition dependent through $h_c \sim 1/(M)^{1/2}$
- Operational pressure range: 0.1 Pa – 100 Pa within which h_c and therefore T are dependent on p. (for $K_n > 1$, i.e. molecular flow)
- High pressure limits: Fig. 2.9, h_c becomes independent of p;
- Low pressure limit: wire thermal conductance dominates heat flow;

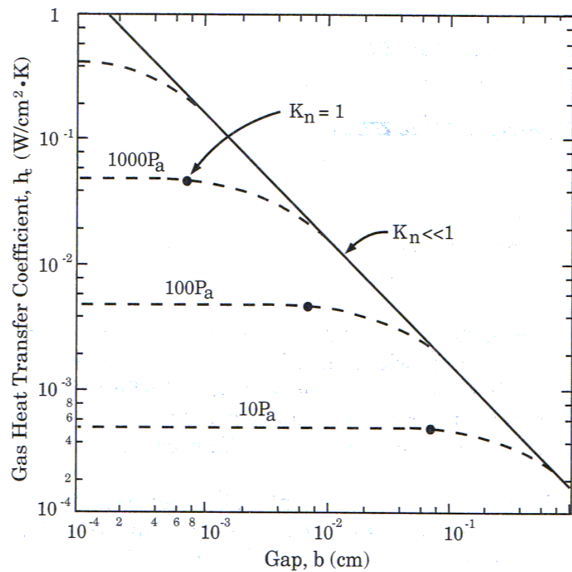
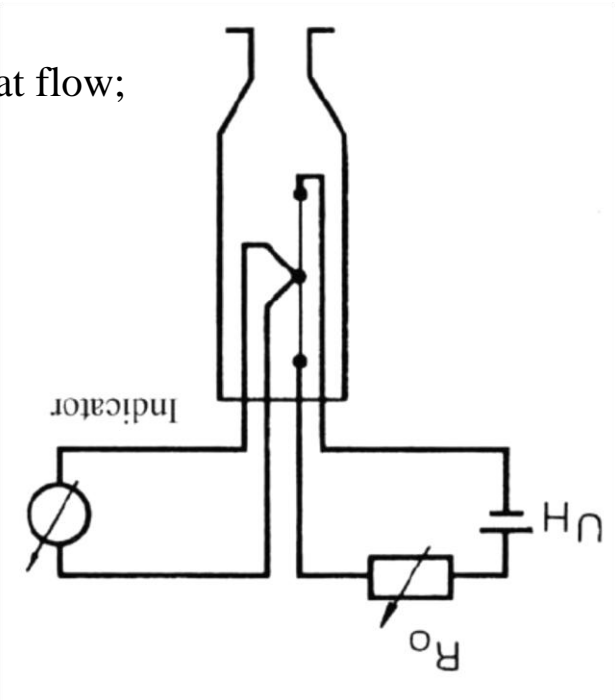
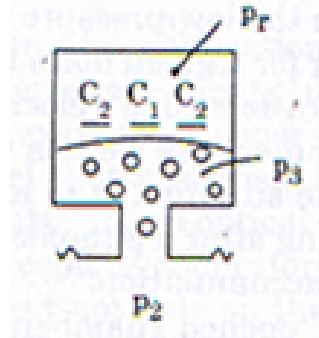


Figure 2.9 Gas-film heat-transfer coefficient, h_c , vs. plate gap, b , for various pressures of Ar. For $Kn \ll 1$, $h_c = K_T/b$, where K_T = bulk thermal conductivity of the gas.





3.5.2. Capacitance diaphragm gauge

- Gas composition independent
- Operational principle: it is based on the bending of a diaphragm that separates the chamber pressure from a sealed vacuum chamber with a ring electrode and a disk electrode in there. The capacitance between the diaphragm and the two fixed electrodes are directly correlated with the amount of warping of the diaphragm, which in turn is related to the pressure differential across the diaphragm.
- Operational pressure range: 10^{-3} Pa – 10^2 Pa
- High pressure limit: mechanical strength of the diaphragm
- Low-pressure limit: thermal expansion of the gauge components caused by temperature fluctuation.

Chapter 4

Evaporation

Subject:

Thermal evaporation of source material and its transport to the substrate in a high-vacuum environment

Most pertinent to PVD;

4.1. Thermodynamics of Evaporation

See Fig. 4.1 for the various thermal evaporation setups.

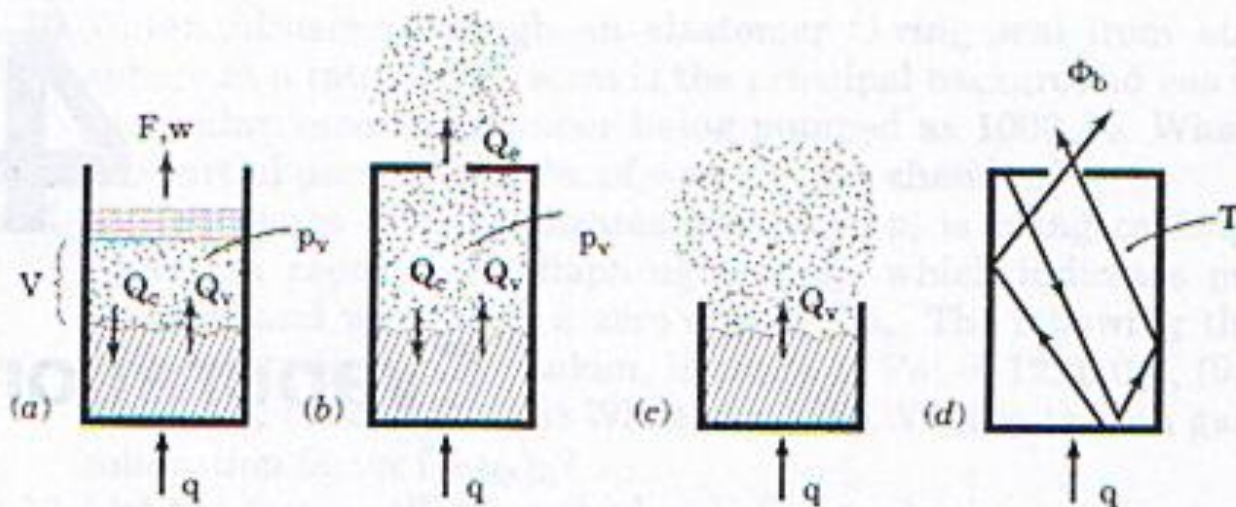


Figure 4.1 Evaporation situations: (a) vapor-liquid (or solid) equilibrium in a closed system, (b) Knudsen-cell effusion, (c) vacuum evaporation, and (d) radiation-blackbody analogy.

4.1.2. Thermodynamics of evaporation processes (consider the setup in fig.4.1(a))

We want to derive a relation between p_v and T .

Along any liquid-vapor or solid-vapor boundary of a phase diagram. We have:

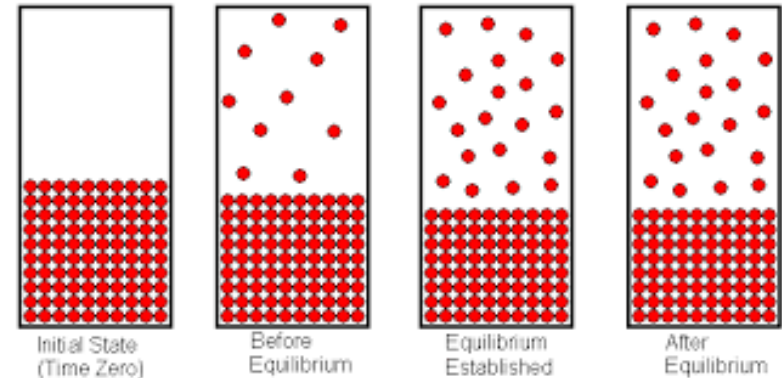
$$\mu_c = \mu_v \quad dG_{mc} = dG_{mv} \quad dG = Vdp - SdT$$

where c and v stand for condensed and vapor phase, respectively.

$$\therefore V_{mc} dp - S_{mc} dT = V_{mv} dp - S_{mv} dT$$

$$\text{or} \quad \frac{dp}{dT} = \frac{S_{mv} - S_{mc}}{V_{mv} - V_{mc}} = \frac{\Delta S_m}{\Delta V_m}$$

Clapeyron equation



Evaporation from a source represents the deviation from such equilibrium in the direction of $\mu_v < \mu_c$, i.e. reduced partial pressure, p . Condensation process represents the opposite, i.e. $\mu_v > \mu_c$, or super saturation, $p > p_v$.

4.1.2. Thermodynamics of evaporation processes (cont'd)

Majority of $\Delta_v H$ goes into liberating the molecule from the condensed phase (fig 4.2).

A small fraction goes into the increase in the translational energy, ϵ_t .

$$\text{At equilibrium: } \because \Delta G_m = \Delta_v H - T\Delta S_m = 0 \quad \therefore \Delta S_m = \frac{\Delta_v H}{T} \quad \therefore \frac{dp}{dT} = \frac{1}{T} \frac{\Delta_v H}{\Delta V_m}$$

Since V_{mc} is typically 1/1000 of V_{mv} , and for ideal gas $V_{mv} = \frac{RT}{p}$

$$\therefore \Delta V_m = V_{mv} - V_{mc} \approx V_{mv} = \frac{RT}{p}$$

$$\therefore \frac{dp}{dT} = \frac{p\Delta_v H}{RT^2}$$

$$\text{or: } \frac{dp}{p} = \frac{\Delta_v H}{RT^2} \bullet dT$$

Clausius-Clapeyron equation

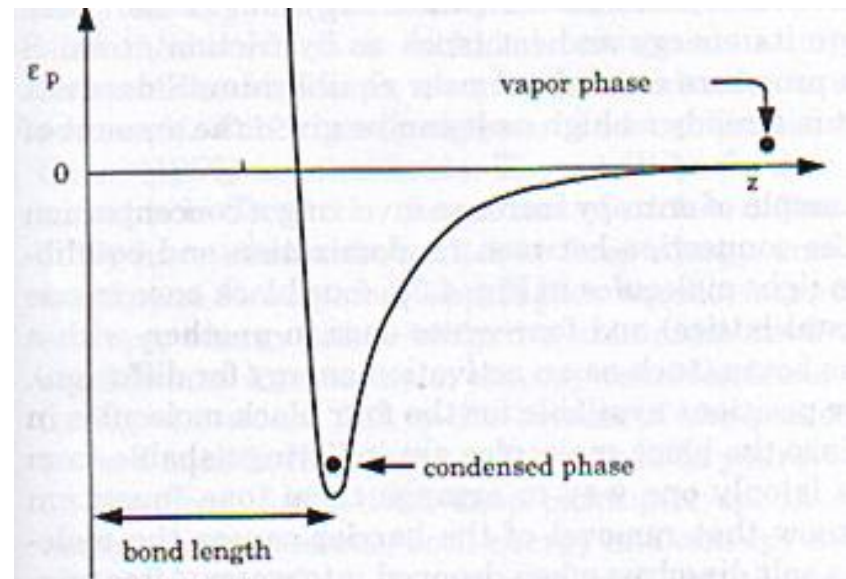
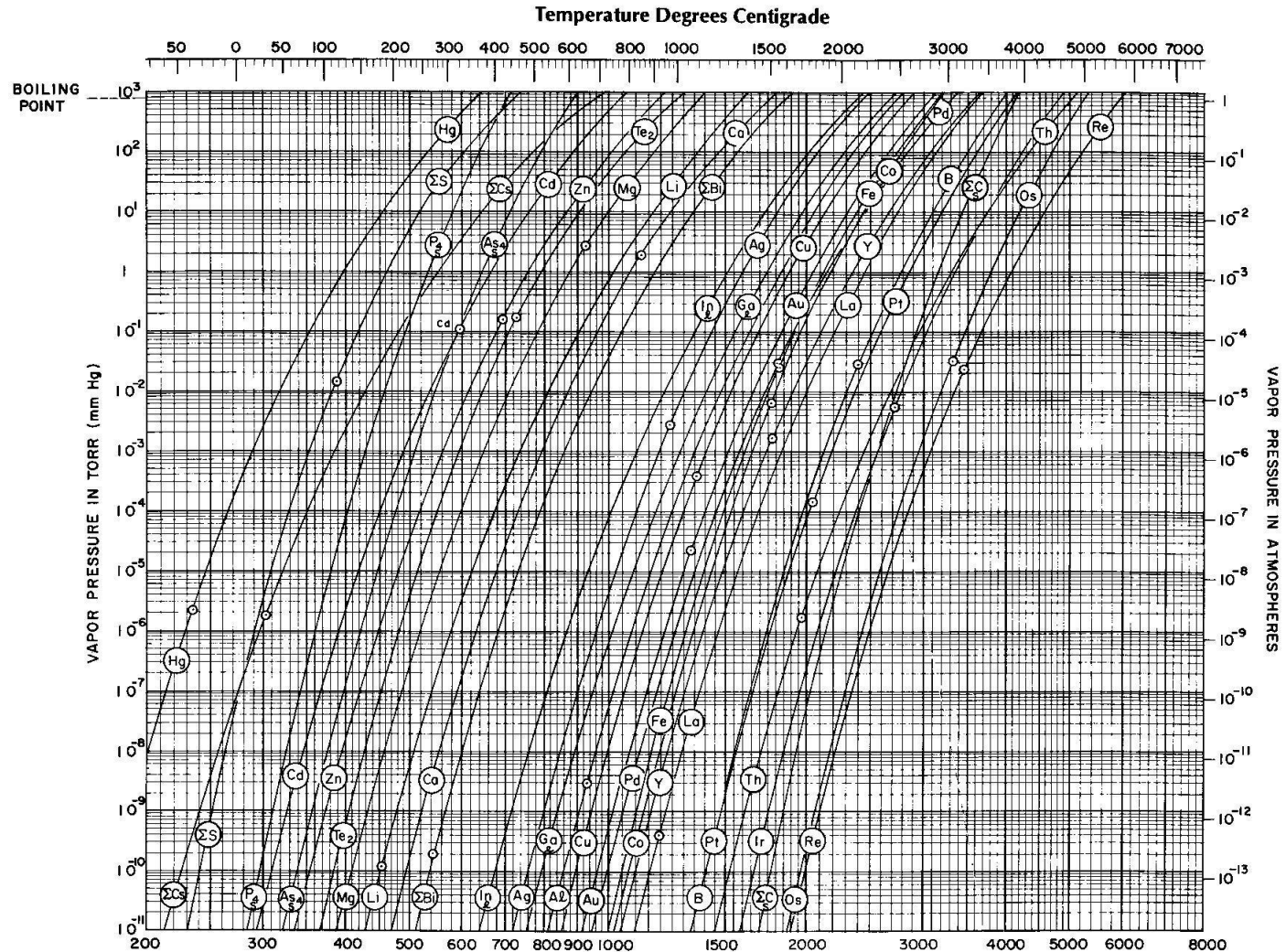


Figure 4.2 Molecular potential-energy diagram for evaporation and condensation.

4.1.2. Thermodynamics of evaporation processes (cont'd)

VAPOR PRESSURE CURVES OF THE ELEMENTS



4.3. The Evaporation of Alloys

Evaporation from a well-mixed alloy **rarely** results in an atomic flux with the same composition as the source alloy. The reason is the different vapor pressure and thus the evaporation rate for different components at a given temperature.

Consider an infinitely miscible alloy B_xC_{1-x} , assume:

$$p_B = a_B p_{vB}$$

and

$$p_C = a_C p_{vC}$$

then

$$\therefore J_i = \frac{1}{4} \frac{N_A p}{RT} \sqrt{\frac{8RT}{\pi M}} = \frac{N_A p}{\sqrt{2\pi MRT}} \left(\frac{mc}{m^2 \cdot \text{sec}} \right) \longrightarrow \frac{J_{vB}}{J_{vC}} = \frac{x}{1-x} \frac{p_{vB}}{p_{vC}} \sqrt{\frac{M_C}{M_B}}$$

where a_B and a_C are the thermodynamic activities that are defined by the ratio of the fugacity of an element in solution to that of the pure element, i.e. the saturated vapor pressure.

4.3. The Evaporation of Alloys

For simplicity we assume the solution being ideal, i.e. $a_B=x_B$ and $a_C=x_C$. It is obvious from this expression that the condition for a proportional evaporation, i.e.

$$\frac{J_{vB}}{J_{vC}} = \frac{x}{1-x}$$

is not satisfied in general *because of the different p's and M's*.

If the alloy is kept uniform throughout the evaporation process, the component with higher vapor pressure will be depleted first. The composition of the atomic flux does not have a steady state. It follows a predictable decay function with time.

If the alloy source is not kept uniform as in most solid source cases, the diffusion of the high-vapor pressure component through the alloy source material determines the composition of the atomic flux, and it is difficult to predict.

The remedy is a continuous feed of an alloy with a different composition into the source.

4.4. Compounds

We limit our discussion to the case of evaporation being in the form of atoms;

Compounds are fundamentally different from alloys in that when the composition is deviating from the few specific values for a given system, precipitation occurs. For the discussion pertinent to evaporation of compound materials, we need to examine in detail the fine structures near the few "specific allowed composition values", and to introduce the concept of [single-phase field](#).

4.4.1. Single-phase field, see Fig. 4.6 of a binary compound.

It represents a finite range of composition around the allowed values (typically within 10^{-4}) within which no precipitation occurs. The composition within that range is varied by the introduction of native defects, i.e., vacancies, interstitials, and anti-sites.

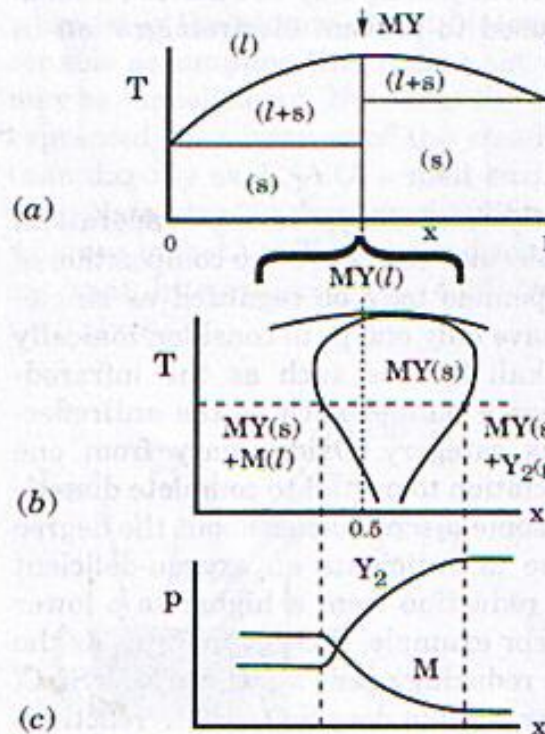


Figure 4.6 General form of phase equilibria for nonstoichiometric binary semiconductors $M_{1-x}Y_x$: (a) T-x projection, (b) T-x projection near $x = 0.5$, and (c) p-x projection. (Source: Reprinted from Ref. 6 with permission. Copyright © 1979, Pergamon Press.)

4.4.2. The importance of Fig. 4.6 (c):

At the two boundaries of the single-phase field, the rich component of the compound precipitates out with its corresponding vapor pressure reaches that of the pure element.

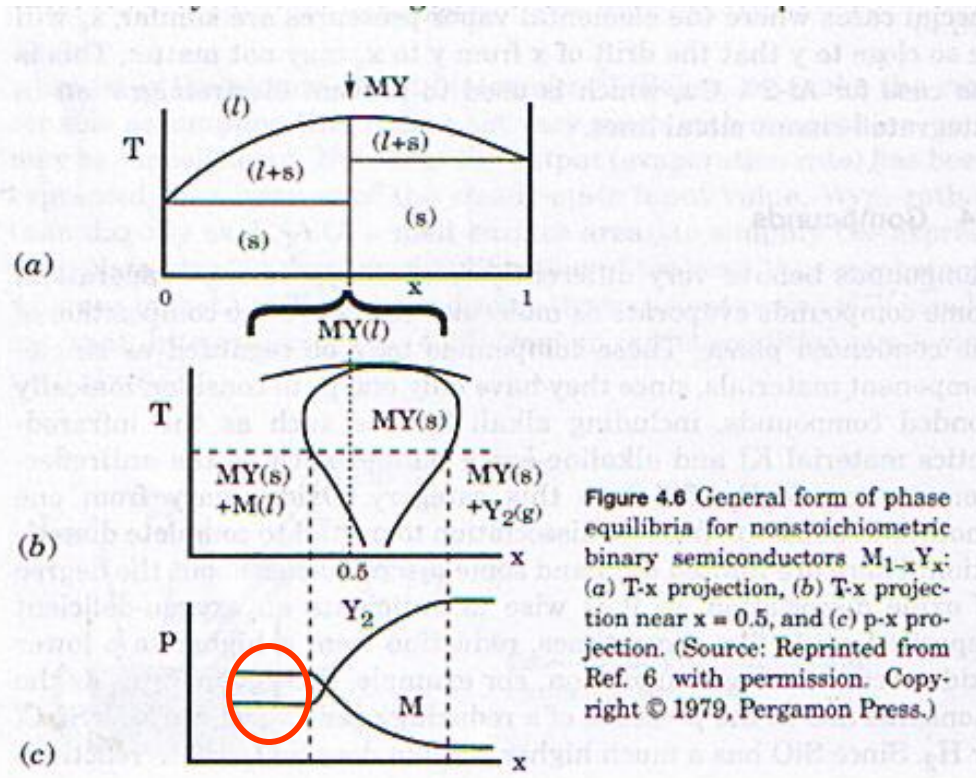


Figure 4.6 General form of phase equilibria for nonstoichiometric binary semiconductors $M_{1-x}Y_x$: (a) T-x projection, (b) T-x projection near $x = 0.5$, and (c) p-x projection. (Source: Reprinted from Ref. 6 with permission. Copyright © 1979, Pergamon Press.)

The vapor pressure curves shift with temperature as shown in Fig. 4.7 for GaAs. For each element, the upper portion of the curve represents the vapor pressure along the phase boundary rich in that element. Beyond 680°C , there is no cross point. Congruent evaporation becomes impossible. Because of the general difference in the evaporation coefficient, α_v , between different elements, congruent evaporation becomes possible at a temperature that is slightly different from the crossover point. Incongruent evaporation results in surface pitting and is undesirable under most circumstances.

Evaporation from separate, single element sources operating at different temperatures is employed when the maximum temperature for congruent evaporation results in an evaporation rate that is too low for the intended application. This is typical for III-V compounds since $p_M < p_Y$ always and p_M is therefore the limiting factor

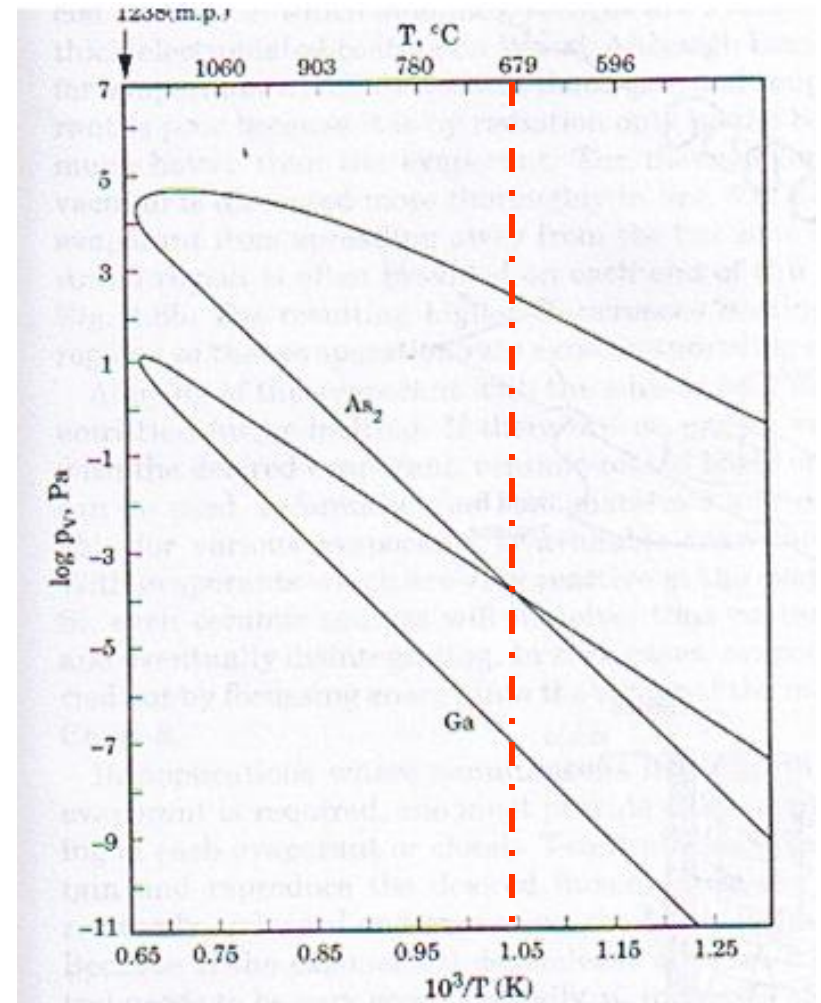


Figure 4.7 Equilibrium vapor pressures of Ga and As_2 along the GaAs liquidus, as functions of T. (Source: Reprinted from Ref. 7 with permission. Copyright © 1979, Pergamon Press. As_1 and As_4 curves deleted.)

4.6. Transport

We consider only the transport in high vacuum, i.e. $K_n > 1$, with the critical dimension L defined by the source-substrate separation which we designate r_0 below.

Using Fig. 4.12 for the following discussion. Consider three types of sources: disc, sphere, and collimated.

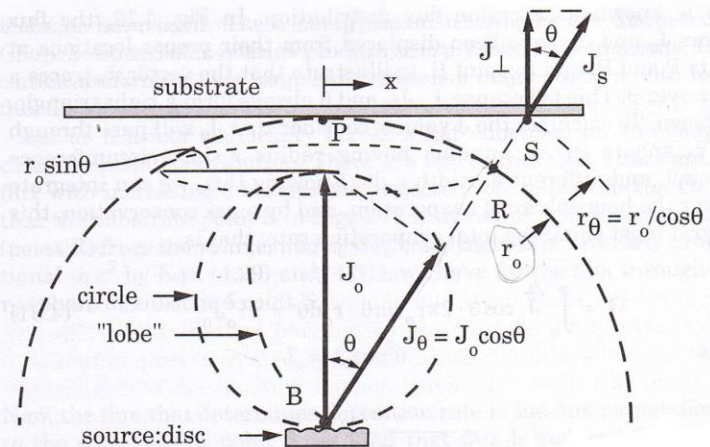


Figure 4.12 Geometry of vacuum evaporation. The flux ratio J_θ/J_0 shown is for the "cosine distribution" characteristic of the disc-shaped source centered at point B; alternate source shapes shown below would have different flux distributions when positioned at B.

4.6. Transport (cont'd)

The following discussion is conceptually simple but easy to make mistakes.

The main issues are arrival uniformity and contamination.

We will discuss the geometrical factors that affect the uniformity of deposition at the substrate.

In the following discussion about flux, we divide the space between the source and the substrate into 3 regions: (1) immediately above the source surface; (2) along the surface of an imaginary sphere touching the substrate at the center, and (3) along and immediately below the substrate surface.

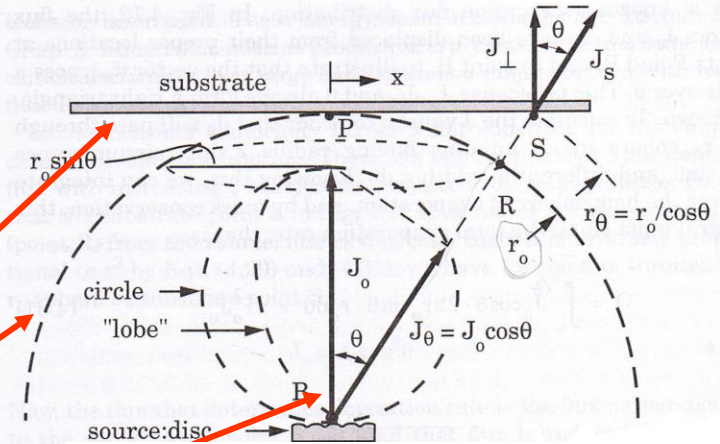


Figure 4.12 Geometry of vacuum evaporation. The flux ratio J_θ/J_o shown is for the "cosine distribution" characteristic of the disc-shaped source centered at point B; alternate source shapes shown below would have different flux distributions when positioned at B.

4.6.2. Disc source: (cont'd)

We are interested in the flux normal to the substrate surface: $J_{\perp} = J_s \cos \vartheta$

Therefore, we have the expression of $J_{(\text{perpendicular})}$ in terms of Q , r_0 , and θ :

$$\begin{aligned} J_{\perp} &= J_s \cos \vartheta = J_{\vartheta} \cos^2 \vartheta \cdot \cos \vartheta = \\ &= J_o \cos \vartheta \cdot \cos^2 \vartheta \cdot \cos \vartheta = J_o \cos^4 \vartheta = \\ &= \frac{Q}{\pi r_o^2} \cos^4 \vartheta \end{aligned}$$

$$J_{\perp} = \frac{Q}{\pi r_o^2} \cos^4 \vartheta$$

